10th ANKARA INTERNATIONAL AEROSPACE CONFERENCE AIAC-2019-041
18-20 September 2019 - METU, Ankara TURKEY

CONTROL OF A FLAPPING WING MICRO AIR VEHICLE FOR NAVIGATION

Özgün Çalış[1]
Middle East Technical University
Ankara, Turkey

Kutluk Bilge Arıkan[2]
TED University
Ankara, Turkey

Dilek Funda Kurtuluş[3]
Middle East Technical University
Ankara, Turkey

ABSTRACT

This paper presents a method to calculate aerodynamic forces and moment of a hawkmoth Manduca sexta wing and to control a flapping wing Micro Air Vehicle (MAV) for navigation. The dynamical model of the MAV is inspired from hawkmoth Manduca sexta and is derived using 6 states. The control inputs are the stroke plane angle and wingbeat frequency. An optimal controller is designed to track the given position reference. It is shown by the simulations that the designed controller satisfies taking-off, hovering, forward motion and the landing.

INTRODUCTION

In order to perform operations that require high maneuverability and quietness, the flapping wing MAVs are convenient due to their small size and agility [Kurtulus, 2011a; Kurtulus, 2011b]. Mathematical aerodynamic modeling of the flapping wing flight and body dynamics are presented by [Deng et al. (2006a)]. Flapping Wing MAV's dynamic characteristics are observed to be unstable in hover [Sun et al. 2005, Sun et al 2007]. This increases the difficulty of control for flapping wing MAV and there is a need to investigate the unsteady aerodynamics of the flapping wing flight in detail in order to model their flight characteristics. Therefore, working on the wing kinematics and morphology of flying insects is an important issue for modelling and designing flapping wing MAVs [Kurtulus et al. 2004, 2005, 2006a, 2006b, 2008; Kurtulus, 2009, Kurtulus, 2018].

In recent years, lots of studies have been carried out for the stabilization and control of flapping wing MAVs [Keennon et al., 2012; Nakatani et al., 2016; Garcia et al., 2003]. Different control methods have been tried for stabilization of flapping wing MAVs [Orlowski et al., 2012]. The desired motion is produced by changing the center of gravity of a butterfly-like flapping wing MAV where PI controller for the pitching angle and PID controller for the roll angle was used. PID controllers are used separately for the pitch and roll controls where the simulations gave satisfactory results in small angle maneuvers. Studies have also been made for altitude control with PID controller [Hines et al., 2011].

[1] M.Sc. Student in Aerospace Engineering of METU, Email: calis.ozgun@.metu.edu.tr
[2] Asst. Prof. Kutluk Bilge ARIKAN, Email: kutluk.arikan@tedu.edu.tr
[3] Prof. Dr. Dilek Funda KURTULUŞ, Email: kurtulus@metu.edu.tr

The nonlinear system was linearized in hover condition and stability studies were performed with state feedback control where the LQR was used [Deng et al. 2006b]. LQR controller is used to stabilize a flapping wing MAV model that is linearized around hover. It is suggested that controller which is designed for hover can also be used to control low forward speeds. It is also stated that under which conditions the weightless wing model is sufficient and under what conditions the weight should not be neglected [Biswal, 2015]. There are some other studies that LQR method is used to calculate state feedback gain [Bhatia et al., 2012].

A non-linear control method is presented by [Rifai et al. (2008)] which shows that linear control methods are not sufficiently robust against external disturbing inputs. In another study, non-linear modeling of a flapping wing MAV was performed where the stability is tested with Lyapunov Method [Banazadeh et al., 2016].

In the current study, the dynamical model is inspired from an insect, namely hawkmoth Manduca sexta and the control is performed by the derivation of the dynamical model using 6 states. The control inputs are the stroke plane angle and wingbeat frequency.

METHOD

In the current study, the altitude is controlled by changing the flapping frequency and the longitudinal motion is controlled by changing the stroke plane angle. Flapping frequency of a hawkmoth Manduca sexta varies between 24.8 Hz and 26.5 Hz at different flight speeds. Especially for the hovering flight, the wingbeat frequency is stated as 26.1 Hz. The stroke plane angle of a hovering Manduca sexta is 15^o while it can get up to 60^o at high forward speeds [Willmott et al., 1997]. The mass of the flapping wing MAV is assumed to be the same with the mass of a hawkmoth Manduca sexta which is approximately 1.456 grams [Kim, 2015]. In order to provide the hover condition of the flapping wing MAV, a flapping motion with 26.1 Hz is selected. But unlike a real hawkmoth Manduca sexta, the stroke plane angle is kept at 22^o at hover. The difference is presumed to be resulted from the assumptions done during the modelling.

Coordinate Definitions

To introduce the wing kinematics 3 different coordinate frames which are Body Fixed Coordinate Frame (X_B,Y_B,Z_B), Global Frame (X_G,Y_G,Z_G) and Wing Fixed Coordinate Frame (X_W,Y_W,Z_W) are shown in Figure 1a and Figure 1b. As shown in Figure 1, Body Fixed Coordinate Frame is fixed to the center of gravity of the body and X_B axis is along the body of the insect. Z_B axis is perpendicular to body and X_B axis. The axis Y_B is pointing out of the page, perpendicular to the X_B and Z_B axes. The Global Frame is fixed at any point on the ground. The X_G axis is pointing the North and the Z_G axis is through the center of the Earth. The Y_G axis is perpendicular to the X_G and Z_G axes and is through to the out of the page. Wing Fixed Coordinate Frame is fixed to the wing root as it is shown in Figure 1b. X_W is along through the chord and Z_W is pointing the wing tip throughout wingspan.

β is the stroke plane angle and θ which is 39.8^o at hover is the body pitch angle in Figure 1a.

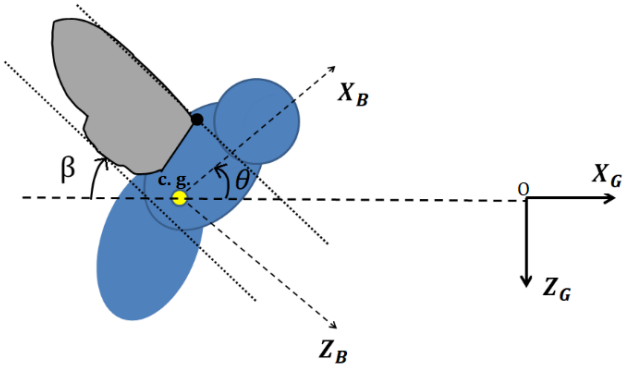

a) Side view

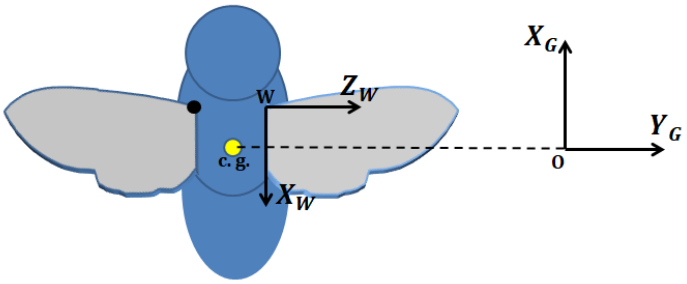

b) Top view

Figure 1 Coordinate definitions and kinematic parameters of the Flapping Wing MAV

Aerodynamic Model

The aerodynamic model used to get lift, drag and rotational forces is based on a quasi-steady model that is proposed by [Kim et al. (2014)]. The translational and rotational forces were considered while added-mass effect and wake-capture were neglected at the quasi-steady approach.

In the current study, the hawkmoth Manduca sexta wing that is used for the aerodynamic model is drawn by attaching the leading edge to the trailing edge where they are both represented via simple functions as shown in Figure 2. The wing is separated into equal pieces along the chord as shown in Figure 2. Total forces and the moment are computed by integrating the lift, the drag and the moment that are created on each strip.

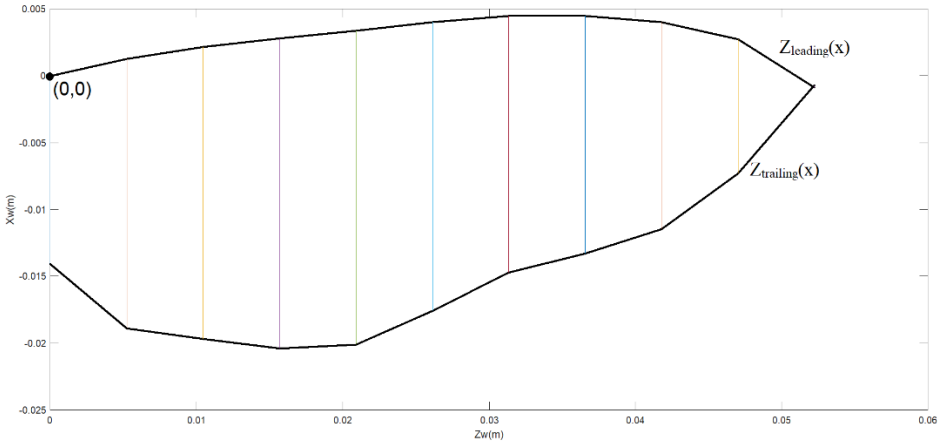

Figure 2 Hawkmoth Manduca sexta wing model (Number of strips = 10)

From the aerodynamic model, the lift, the drag and the moment around the root at (0,0) point of the wing is obtained (Figure 2). Vertical, horizontal and rotational forces acting on the center of gravity of the flapping wing MAV are obtained by translating these forces to the Global Frame.

In order to obtain enough vertical force that supports the weight of the flapping wing MAV, which is one of the main objectives, the model is evaluated. As a first step a strip refinement study is performed to check the number of strip effects on the aerodynamics forces. Six different cases are compared with respect to number of strips = 25, 50, 75, 100, 125 and 150 as shown in Figure 4.

For the simulations, the kinematics used are given in Eq. 1 to Eq.6 which are taken from [Kim et al. (2014)].

$$\varphi(t) = \varphi_{amp} sin(2\pi f t) \tag{1}$$

$$\dot{\varphi}(t) = \varphi_{amp} \cdot (\pi/180)(2\pi f) cos(2\pi f t) \tag{2}$$

$$\theta(t) = \theta_{amp} sin(2\pi f t) \tag{3}$$

$$\dot{\theta}(t) = \theta_{amp} \cdot (\pi/180)(2\pi f) cos(2\pi f t) \tag{4}$$

$$\alpha(t) = \frac{\alpha_{amp}}{\tanh(C_\alpha)} \cdot \tanh(C_\alpha \cdot \sin(2\pi f t + \psi_\alpha)) + \alpha_0 \tag{5}$$

$$\dot{\alpha}(t) = \frac{\alpha_{amp}}{\tanh(C_\alpha)} \cdot (\pi/180)(2\pi f) \cdot [1 - (\tanh(C_\alpha \cdot \sin(2\pi f t + \psi_\alpha)))^2] \cdot (C_\alpha \cdot \cos(2\pi f t + \psi_\alpha)) \tag{6}$$

In the current study,

$$\varphi_{amp} = -55.4°$$
$$\theta_{amp} = 0°$$
$$\alpha_{amp} = 45°$$
$$\alpha_0 = 90°$$
$$f = 26.1 \text{ Hz}$$
$$C_\alpha = 4.5$$
$$\psi_\alpha = -\frac{\pi}{2}$$

The wing kinematics used for calculations is shown in Figure 3a and Figure 3b.

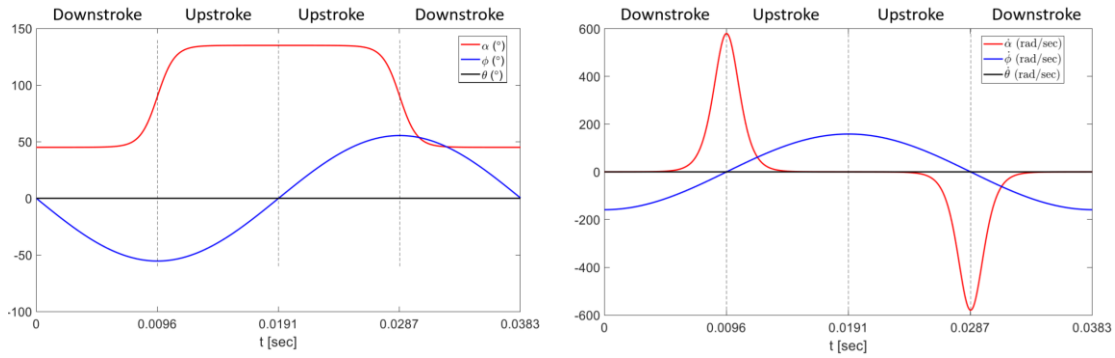

Figure 3 a) Angular positions of the wing with respect to time during one period b) Angular velocities of the wing with respect to time during one period

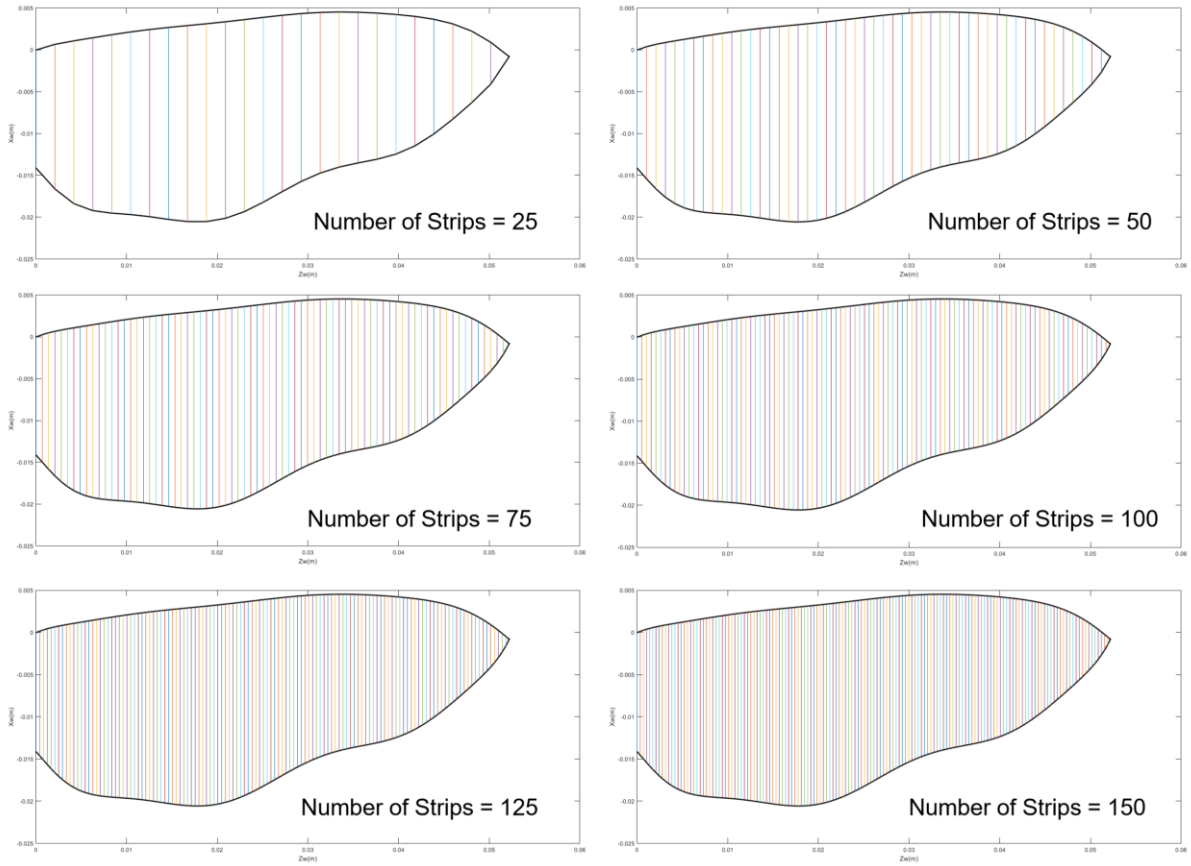

Figure 4 Representation of the hawkmoth Manduca sexta wing model based on different number of strips

As the number of strips is increased, the created vertical force converges to a maximum value which is enough to lift a hawkmoth Manduca sexta as represented in Figure 5. The convergence is obtained after 125 strips. The case with the number of strips of 150 creates 0.014298 Newton which is found to be satisfactory in order to support the weight of the flapping wing MAV which is assumed to have the same mass with a hawkmoth Manduca sexta.

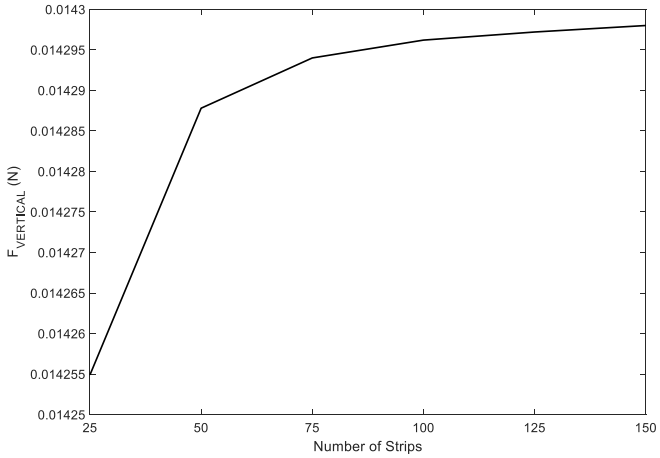

Figure 5 Mean vertical force versus number of strips

The vertical and horizontal forces at 22 degrees stroke plane angle are shown in Figure 6.

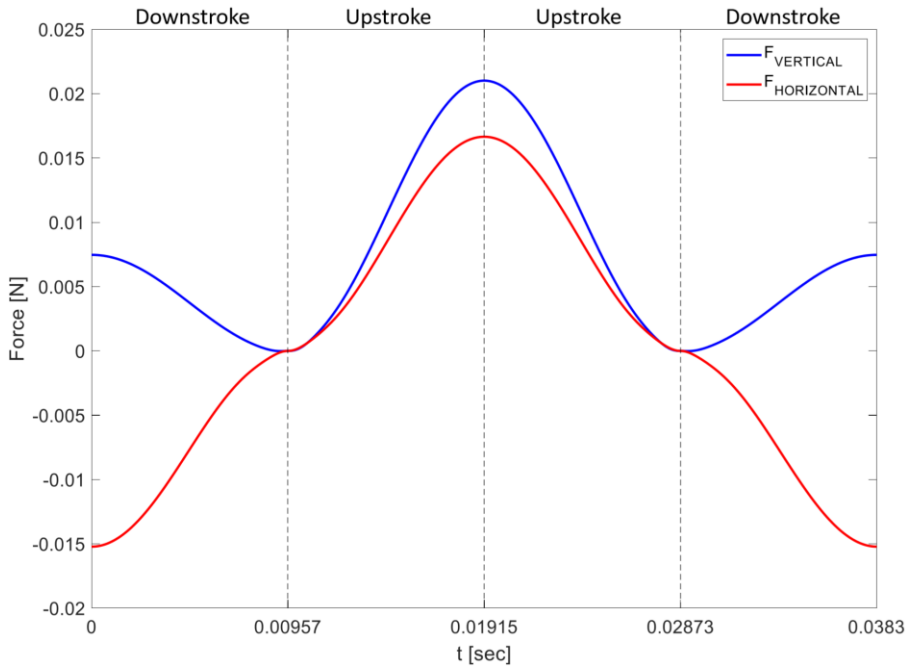

Figure 6 Vertical and horizontal forces with respect to time for one period

Vertical and horizontal forces obtained with different stroke planes angles are shown in Figure 7 and Figure 8

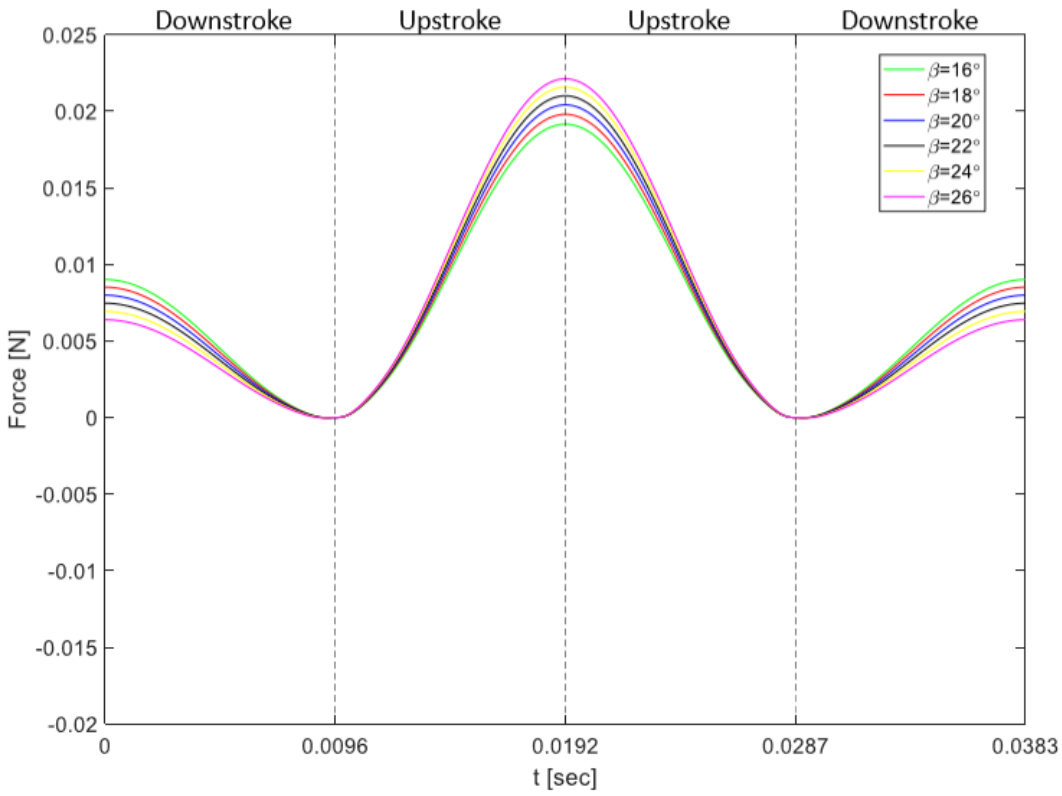

Figure 7 Vertical forces for different stroke plane angles with respect to time for one period

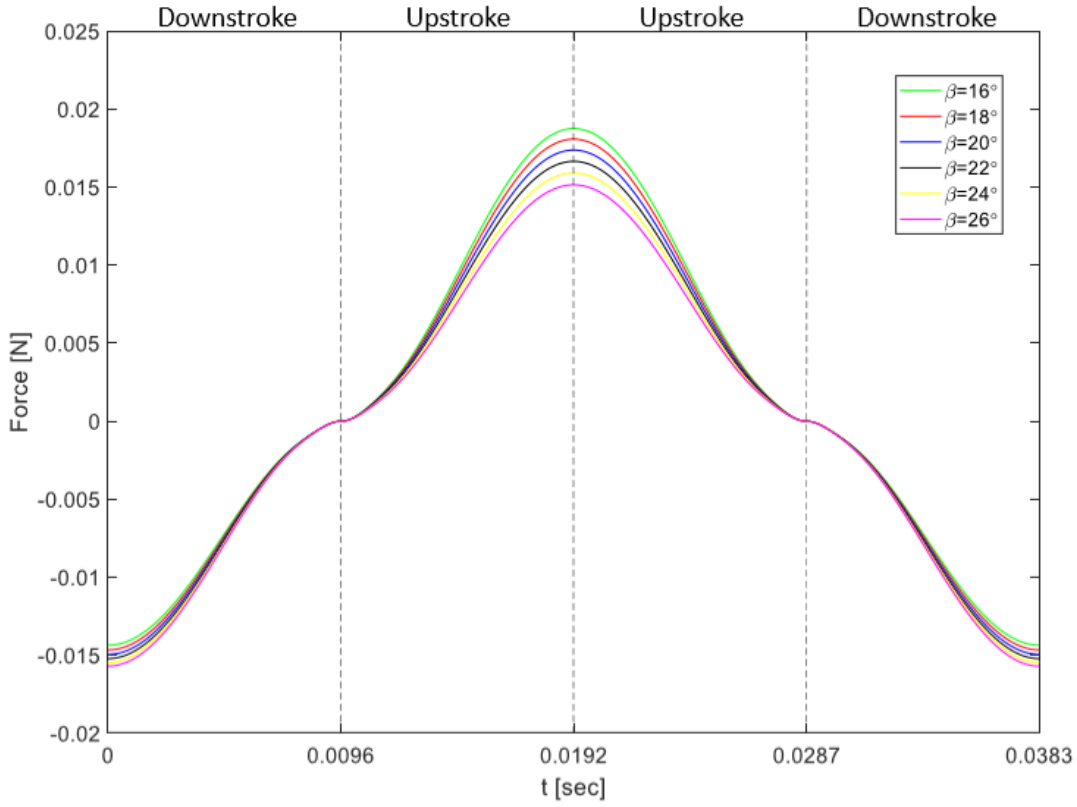

Figure 8 Horizontal forces for different stroke plane angles with respect to time during one period

System Modelling

The forces and moments created by the flapping of the wing were applied to the wing root. The distance between the wing root and the center of mass of the MAV acts as moment arm and the pitching movement occurs. The forces F_{XB}, F_{ZB} and the moment M_{YB} includes the aerodynamic forces and moment. The LTI model is obtained for hovering condition.

The 2D flight of a flapping wing MAV is studied and velocity components are obtained as Eq. (7).

$$\vec{V} = \dot{X}_B\vec{\imath} + \dot{Z}_B\vec{k} = u\vec{\imath} + w\vec{k} \tag{7}$$

When the time-dependent derivative of the body velocity is achieved, the body accelerations a_{XB} and a_{ZB} are found as shown at Eq. (8).

$$\dot{\vec{V}} = (\dot{u} + wq)\vec{\imath} + (\dot{w} - uq)\vec{k} \tag{8}$$

where, a_{XB} is the acceleration of the body in X_B direction and a_{ZB} is the acceleration of the body in Z_B direction.

$$a_{XB} = \dot{u} + wq \tag{9}$$

$$a_{ZB} = \dot{w} + uq \tag{10}$$

Total forces acting on the body is equal to the mass times acceleration. Similarly total moment acting on the center of gravity is equal to the moment of inertia times angular velocity. $\dot{u}, \dot{w}$ and $\dot{q}$ are found as shown between Eq. (11) and Eq. (13)

$$\dot{u} = -wq + F_{XB} - gsin\theta \tag{11}$$

$$\dot{w} = uq + gcos\theta - F_{ZB} \tag{12}$$

$$\dot{q} = \frac{M_{YB}}{J_Y} \tag{13}$$

Six state equations are obtained as shown in Eq. (14) to Eq. (19).

$$\dot{x_1} = x_2 = \dot{X}_B = ucos\theta - wsin\theta \tag{14}$$

$$\dot{x_2} = \ddot{x_1} = \ddot{X}_B = \frac{F_{XB}}{m}cos\theta + \frac{F_{ZB}}{m}sin\theta - 2gsin\theta cos\theta \tag{15}$$

$$\dot{x_3} = x_4 = \dot{Z}_B = usin\theta + wcos\theta \tag{16}$$

$$\dot{x_4} = \ddot{x_3} = \ddot{Z}_B = \frac{F_{XB}}{m}\sin\theta - \frac{F_{ZB}}{m}cos\theta - gsin^2\theta + g cos^2\theta \tag{17}$$

$$\dot{x_5} = x_6 = q \tag{18}$$

$$\dot{x_6} = \ddot{x_5} = \dot{q} = \frac{M_{YB}}{J_Y} \tag{19}$$

The System Matrix A is achieved by Jacobian Matrix Method. Derivatives of all the six state equations from Eq. 14 to Eq. 19 with respect to each of the six state variables $x = [x_B\ \dot{x_B}\ z_B\ \dot{z_B}\ \theta\ q]^T$ are obtained. The result is 6 by 6 linearized System Matrix A as shown in Eq. (20)

$$A = \begin{bmatrix} 0 & \cos\theta & 0 & -\sin\theta & -u\sin\theta - w\cos\theta & 0 \\ 0 & \frac{\partial \delta F_{XB}}{\partial \delta u}\cos\theta + \frac{\partial \delta F_{ZB}}{\partial \delta u}\sin\theta & 0 & \frac{\partial \delta F_{XB}}{\partial \delta w}\cos\theta + \frac{\partial \delta F_{ZB}}{\partial \delta w}\sin\theta & \frac{\partial \delta F_{XB}}{\partial \delta \theta}\cos\theta - F_{XB}\sin\theta + \frac{\partial \delta F_{ZB}}{\partial \delta \theta}\sin\theta + F_{ZB}\cos\theta - 2g(\cos\theta - \sin\theta) & \frac{\partial \delta F_{XB}}{\partial \delta q}\cos\theta + \frac{\partial \delta F_{ZB}}{\partial \delta q}\sin\theta \\ 0 & \sin\theta & 0 & \cos\theta & u\cos\theta - w\sin\theta & 0 \\ 0 & \frac{\partial \delta F_{XB}}{\partial \delta u}\sin\theta - \frac{\partial \delta F_{ZB}}{\partial \delta u}\cos\theta & 0 & \frac{\partial \delta F_{XB}}{\partial \delta w}\sin\theta - \frac{\partial \delta F_{ZB}}{\partial \delta w}\cos\theta & \frac{\partial \delta F_{XB}}{\partial \delta \theta}\sin\theta + F_{XB}\cos\theta - \frac{\partial \delta F_{ZB}}{\partial \delta \theta}\cos\theta + F_{ZB}\sin\theta & \frac{\partial \delta F_{XB}}{\partial \delta q}\sin\theta - \frac{\partial \delta F_{ZB}}{\partial \delta q}\cos\theta \\ 0 & 0 & 0 & 0 & 0 & 1 \\ 0 & \frac{\partial \delta M_{YB}}{\partial \delta u} & 0 & \frac{\partial \delta M_{YB}}{\partial \delta w} & \frac{\partial \delta M_{YB}}{\partial \delta \theta} & \frac{\partial \delta M_{YB}}{\partial \delta q} \end{bmatrix} \tag{20}$$

RESULTS

Stability Analysis and Stabilization

At this stage numerical values of System Matrix A that are proposed by [Lee et al. (2014)] are used. The System Matrix A that is used for the stability analysis and controller design is shown in Eq. (21).

$$A = \begin{bmatrix} 0 & 1 & 0 & 0 & 0 & 0 \\ 0 & -1.7008 & 0 & -0.4986 & -7.5291 & -0.0009 \\ 0 & 0 & 0 & 1 & 0 & 0 \\ 0 & -1.6286 & 0 & -1.8916 & -6.2730 & -0.0005 \\ 0 & 0 & 0 & 0 & 0 & 1 \\ 0 & -351.4311 & 0 & 205.7584 & 0 & -0.7916 \end{bmatrix} \tag{21}$$

Two of the eigenvalues of the open loop system is located on the positive side of the real axis so the system has unstable dynamic characteristics Eq. (22).

$$\lambda = \begin{bmatrix} 0 \\ 0 \\ -16.9804 \\ 6.7527 + 13.6469i \\ 6.7527 - 13.6469i \\ -0.9089 \end{bmatrix} \tag{22}$$

In order to calculate the Control Matrix B, derivatives of the six state equations between Eq. (14) and Eq. (19) with respect to the control variables that are control input angle (*β*) and wingbeat frequency (*f*) are obtained. The 6 by 2 Control Matrix B is created with the results.

Control Matrix B is obtained by calculating the changes of the 6 state equations according to the control input angle (*β*) and wingbeat frequency (*f*) Eq. (23).

$$\mathrm{B} = \begin{bmatrix} 0 & 0 \\ \partial\delta\mathrm{F_{XB}}/\partial\delta\beta \cos\theta + \partial\delta\mathrm{F_{ZB}}/\partial\delta\beta \sin\theta & \partial\delta\mathrm{F_{XB}}/\partial\delta\mathrm{f} \cos\theta + \partial\delta\mathrm{F_{ZB}}/\partial\delta\mathrm{f} \sin\theta \\ 0 & 0 \\ \partial\delta\mathrm{F_{XB}}/\partial\delta\beta \sin\theta - \partial\delta\mathrm{F_{ZB}}/\partial\delta\beta \cos\theta & \partial\delta\mathrm{F_{XB}}/\partial\delta\mathrm{f} \sin\theta - \partial\delta\mathrm{F_{ZB}}/\partial\delta\mathrm{f} \cos\theta \\ 0 & 0 \\ \partial\delta\mathrm{M_{YB}}/\partial\delta\beta & \partial\delta\mathrm{M_{YB}}/\partial\delta\mathrm{f} \end{bmatrix} \tag{23}$$

The numerical values that are proposed by [Lee et al. (2014)] are used at this stage and the Matrix B is shown as Eq. (24).

$$\mathrm{B} = \begin{bmatrix} 0 & 0 \\ 7.73 & 0.51 \\ 0 & 0 \\ 6.6 & -0.59 \\ 0 & 0 \\ -686.52 & -0.55 \end{bmatrix} \tag{24}$$

Algebraic Riccati Equation is solved to calculate the feedback gain by aiming to minimize the cost function Eq. (25).

$$J = \frac{1}{2}\int_0^\infty \left(x_B^T F x_B + u_b^T G u_b\right) dt \tag{25}$$

The weight matrixes F and G are chosen as Eq. (26) and Eq. (27) to minimize the Cost Function J [Lee et al. (2014)].

$$F = \begin{bmatrix} 10 & 0 & 0 & 0 & 0 & 0 \\ 0 & 1 & 0 & 0 & 0 & 0 \\ 0 & 0 & 10 & 0 & 0 & 0 \\ 0 & 0 & 0 & 1 & 0 & 0 \\ 0 & 0 & 0 & 0 & 10 & 0 \\ 0 & 0 & 0 & 0 & 0 & 1 \end{bmatrix} \tag{26}$$

$$G = \begin{bmatrix} 0.01 & 0 \\ 0 & 0.041 \end{bmatrix} \tag{27}$$

After the full state feedback is applied to the system, all the six states became stable as shown in Figure 9.

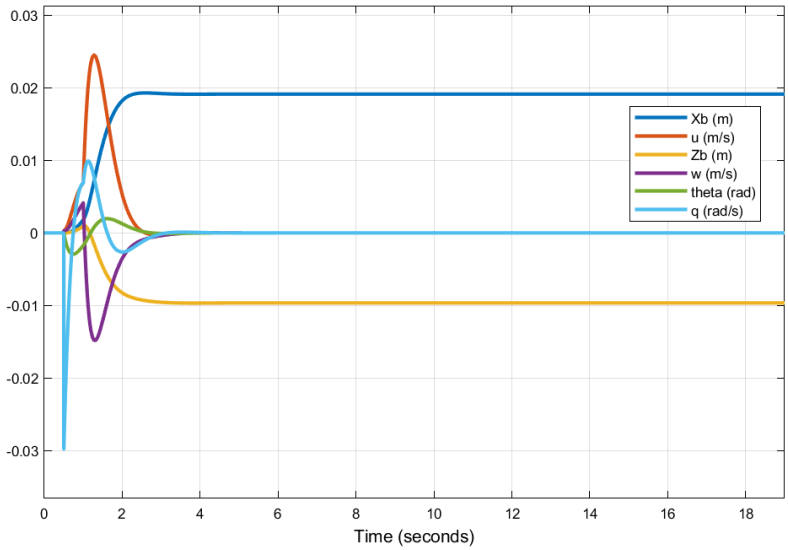

Figure 9 Closed loop system response of the flapping wing MAV model

Tracking Controller

In order to make the system states to come to the desired values, an integral tracker has been designed to track the reference value. Reference inputs are given for forward and upward movement to the LTI system that is modelled for hover. The input value is such that Flapping Wing MAV will move to a height of 1 meter during 2 seconds and after staying in the hover condition at this height for 3 seconds, to move 5 meters forward. After staying in the hover condition again for 3 seconds, the Flapping Wing MAV will land on the ground in 2 seconds. The reference inputs and the responses of the system are given in Figure 10a and Figure 10b.

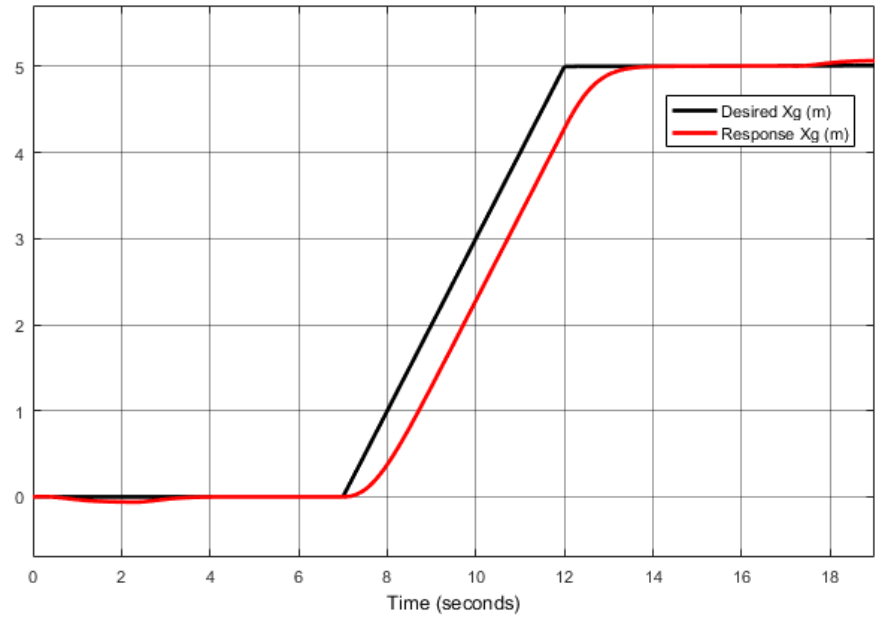

a) The desired X_G input and the X_G response of the system.

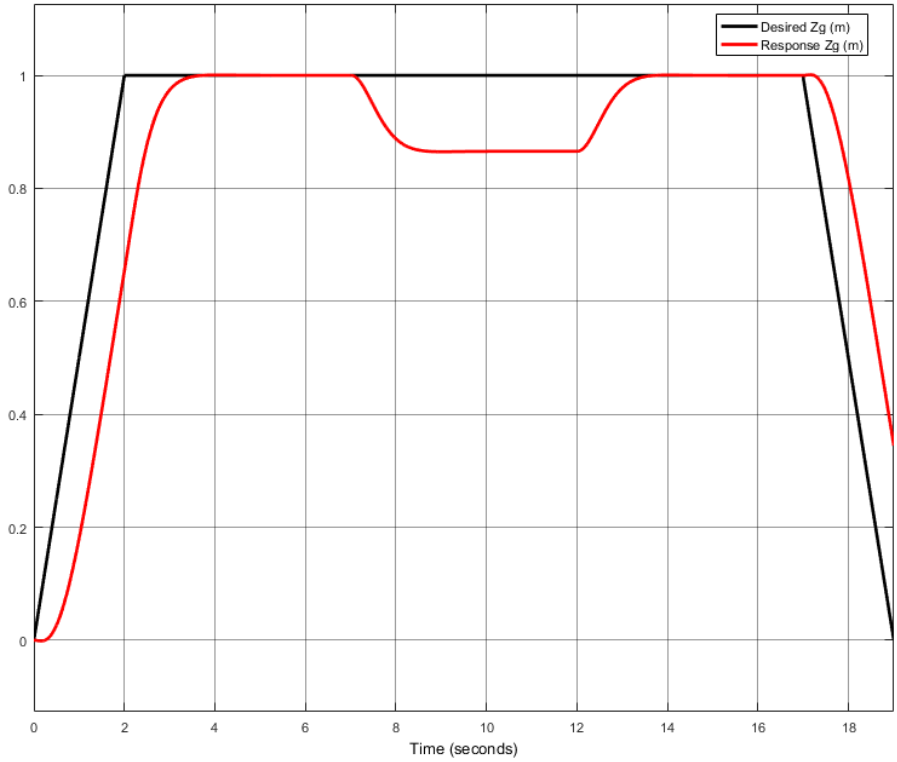

b) The desired Z_G input and the Z_G response of the system.

Figure 10 Responses of the system to reference inputs

In order to track the reference X_G, the error is tried to be reduced to zero. Consequently a deterioration occurs at Z_G output between seconds 7 and 13 as shown in Figure 10b.

Conclusion

The dynamical model of a hawkmoth Manduca sexta insect is derived using 6 states. LQR controller is found to be proper to stabilize a Flapping Wing MAV at hover condition. The controller which is designed for the hover condition is tested at low speed flights and the simulation was able to track the reference inputs. Calculations and simulations have been made in Matlab and Matlab/Simulink.

Acknowledgement

This work is supported by TUBITAK Project no: 116M273

References

Banazadeh, A., & Taymourtash, N. (2016). Adaptive attitude and position control of an insect-like flapping wing air vehicle. *Nonlinear Dynamics, 85*(1), 47-66.

Bhatia, M., Patil, M., Woolsey, C., Stanfordx, B., & Beran, P. (2012, August). Lqr controller for stabilization of flapping wing mavs in gust environments. In *AIAA Atmospheric Flight Mechanics Conference* (p. 4867).

Biswal, S. (2015). Modeling and Control of Flapping Wing Micro Aerial Vehicles. Arizona State University.

Deng, X., Schenato, L., Wu, W. C., & Sastry, S. S. (2006a). Flapping flight for biomimetic robotic insects: Part I-system modeling. IEEE Transactions on Robotics, *22*(4), 776-788.

Deng, X., Schenato, L., & Sastry, S. S. (2006b). Flapping flight for biomimetic robotic insects: Part II-flight control design. IEEE Transactions on Robotics, *22*(4), 789-803.

Garcia, H., Abdulrahim, M., & Lind, R. (2003, August). Roll control for a micro air vehicle using active wing morphing. In AIAA Guidance, Navigation, and Control Conference and Exhibit(p. 5347).

Hines, L. L., Arabagi, V., & Sitti, M. (2011, May). Free flight simulations and pitch and roll control experiments of a sub-gram flapping-flight micro aerial vehicle. In *2011 IEEE International Conference on Robotics and Automation* (pp. 1-7). IEEE.

Keennon, M., Klingebiel, K., & Won, H. (2012, January). Development of the nano hummingbird: A tailless flapping wing micro air vehicle. In *50th AIAA aerospace sciences meeting including the new horizons forum and aerospace exposition* (p. 588)

Kim, J. K., & Han, J. H. (2014). A multibody approach for 6-DOF flight dynamics and stability analysis of the hawkmoth Manduca sexta. *Bioinspiration & biomimetics*, *9*(1), 016011.

Kim, J. K., Han, J. S., Lee, J. S., & Han, J. H. (2015). Hovering and forward flight of the hawkmoth Manduca sexta: trim search and 6-DOF dynamic stability characterization. Bioinspiration & biomimetics, *10*(5), 056012.

Kurtulus D.F. (2009) Vortex topology on a flapping airfoil. Proceeding of International Symposium on Light Weight Unmanned Aerial Vehicle Systems and Subsystems, UAS LW 2009, Oostend Belgium, 11-13 March, 2009.

Kurtulus D.F. (2018) Aerodynamic loads of small amplitude pitching NACA 0012 airfoil at Reynolds Number of 1000, AIAA Journal, Vol. 56, No. 8, pp. 3328-3331.

Kurtulus D.F., Farcy A., Alemdaroglu N. (2004) Numerical Calculation and Analytical Modelization of Flapping Motion, Proceeding of 1 st European Micro Air Vehicle Conference and Flight Competition. Braunschweig, Germany, 13-14 July 2004.

Kurtulus D. F., Farcy A., Alemdaroglu N. (2005) Unsteady Aerodynamics of Flapping Airfoil in Hovering Flight at Low Reynolds Numbers, 43rd AIAA Aerospace Sciences Meeting and Exhibit, Reno, Nevada, USA, 10-13 January 2005.

Kurtulus D. F., David L., Farcy A., Alemdaroglu N. (2006a) A Parametrical Study with Laser Sheet Visualization for an Unsteady Flapping Motion, 36th AIAA Fluid Dynamics Conference and Exhibit, San Francisco, California, USA, 5-8 June 2006.

Kurtulus D. F., David L., Farcy A., Alemdaroglu N. (2008) Aerodynamic Characteristics of Flapping Motion in Hover, Experiments in Fluids, Vol. 44, No. 1, p: 23–36, January 2008.

Kurtulus D. F., David L., Farcy A., Alemdaroglu N. (2006b) *Laser Sheet Visualization for Flapping Motion in Hover*, 44rd AIAA Aerospace Sciences Meeting and Exhibit, Reno, Nevada, USA, 9-12 January 2006

Kurtulus D. F. (2011a) *Introduction to Micro Air Vehicles: Concepts, Design and Applications*, Recent Developments in Unmanned Aircraft Systems (UAS, including UAV and MAV), VKI LS 2011-04, ISBN-13 978-2-87516-017-1, p: 1-30, April 2011.

Kurtulus D.F. (2011b) *Unsteady Aerodynamics of Flapping Aerofoils: Case Studies with Experimental, Numerical, Theoretical and Soft Computing Methods*, Recent Developments in Unmanned Aircraft Systems (UAS, including UAV and MAV), VKI LS 2011-04, ISBN-13 978-2-87516-017-1, p: 1-36, April 2011.

Lee, J. S., Kim, J. K., & Han, J. H. (2014). Stroke plane control for longitudinal stabilization of hovering flapping wing air vehicles. *Journal of Guidance, Control, and Dynamics*, *38*(4), 800-806.

Nakatani, Y., Suzuki, K., & Inamuro, T. (2016). Flight control simulations of a butterfly-like flapping wing–body model by the immersed boundary–lattice Boltzmann method. *Computers & Fluids*, *133*, 103-115.

Orlowski, C. T., & Girard, A. R. (2012). Dynamics, stability, and control analyses of flapping wing micro-air vehicles. *Progress in Aerospace Sciences*, *51*, 18-30.

Rifai, H., Marchand, N., & Poulin, G. (2008, May). Bounded control of a flapping wing micro drone in three dimensions. In *2008 IEEE International Conference on Robotics and Automation* (pp. 164-169). IEEE.

Sun, M., & Xiong, Y. (2005). Dynamic flight stability of a hovering bumblebee. *Journal of experimental biology*, *208*(3), 447-459.

Sun, M., Wang, J., & Xiong, Y. (2007). Dynamic flight stability of hovering insects. *Acta Mechanica Sinica*, *23*(3), 231-246.

Willmott, A. P., and Ellington, C. P. (1997). The mechanics of flight in the hawkmoth Manduca sexta. I. Kinematics of hovering and forward flight. *Journal of experimental Biology*, *200*(21), 2705-2722.